

Analytical Methods

Accepted Manuscript



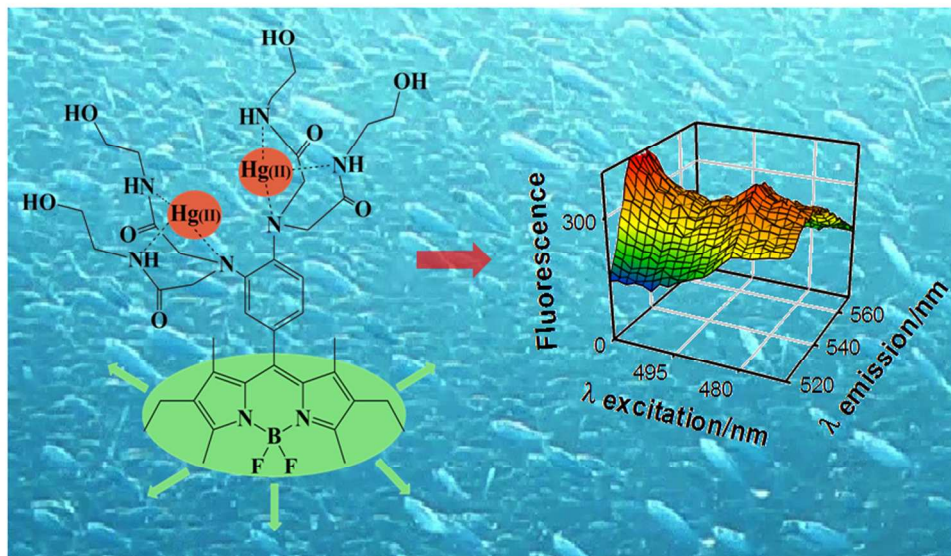
This is an *Accepted Manuscript*, which has been through the Royal Society of Chemistry peer review process and has been accepted for publication.

Accepted Manuscripts are published online shortly after acceptance, before technical editing, formatting and proof reading. Using this free service, authors can make their results available to the community, in citable form, before we publish the edited article. We will replace this *Accepted Manuscript* with the edited and formatted *Advance Article* as soon as it is available.

You can find more information about *Accepted Manuscripts* in the [Information for Authors](#).

Please note that technical editing may introduce minor changes to the text and/or graphics, which may alter content. The journal's standard [Terms & Conditions](#) and the [Ethical guidelines](#) still apply. In no event shall the Royal Society of Chemistry be held responsible for any errors or omissions in this *Accepted Manuscript* or any consequences arising from the use of any information it contains.

1
2
3
4
5
6
7
8
9
10
11
12
13
14
15
16
17
18
19
20
21
22
23
24
25
26
27
28
29
30
31
32
33
34
35
36
37
38
39
40
41
42
43
44
45
46
47
48
49
50
51
52
53
54
55
56
57
58
59
60



254x190mm (96 x 96 DPI)

1
2
3
4
5
6
7 **Second-order fluorimetric approach based on a boron**
8
9
10 **dipyrromethene (BODIPY) tetraamide derivative for**
11
12
13 **Hg(II) chemosensing in water and fish samples**
14
15
16
17
18
19
20

21 Valeria A. Lozano,^a Arsenio Muñoz de la Peña,^{b,*} Graciela M. Escandar^{a,*}
22
23
24
25
26

27 ^a *Instituto de Química Rosario (CONICET–UNR), Facultad de Ciencias Bioquímicas y*
28 *Farmacéuticas, Universidad Nacional de Rosario, Suipacha 531 (2000) Rosario,*
29 *Argentina.*
30
31
32

33 ^b *Department of Analytical Chemistry, University of Extremadura, 06006, Badajoz,*
34 *España.*
35
36
37
38
39
40
41
42
43
44
45
46
47
48
49
50
51
52
53

54
55 * Corresponding authors. Tel/fax: 0054-341-4372704 (G. Escandar), E-mail addresses:
56 arsenio@unex.es (A. Muñoz de la Peña), escandar@iquir-conicet.gov.ar (G. Escandar)
57
58
59
60

1
2
3 A new fluorimetric method is described for the determination of Hg(II), based on the
4 selectivity of a boron dipyrromethene tetraamide derivative (BODIPYTD) towards this
5 ion, in combination with second-order chemometric analysis, to deal with matrix
6 interferences. This is the first time that the selectivity of a mercury chemosensor
7 regarding other metal ions is reinforced with the selectivity offered by second-order
8 calibration, which is able to overcome the potential interference produced by organic
9 constituents of natural or bio-samples. After the BODIPYTD-Hg(II) complex was
10 formed, the excitation-emission fluorescence matrix was recorded and parallel factor
11 analysis (PARAFAC) was applied for data processing. This algorithm achieves the
12 second-order advantage and was able to overcome the problem of the presence of
13 unexpected interferences. The method was applied to the direct determination of Hg(II)
14 ion in environmental waters and fish muscle tissues, with minimal pretreatment steps
15 and without the need of organic solvents. The results were successfully evaluated
16 through a spiking recovery study in both types of real samples, which have constituents
17 displaying fluorescence signals potentially able to interfere in the analysis. This latter
18 fact demonstrates the excellent selectivity of the proposed method. The studied
19 concentration range in water samples was 10-30 ng mL⁻¹, while in fish samples it was
20 0.12-0.30 µg g⁻¹. The limits of detection for water and fish samples were 2 ng mL⁻¹ and
21 4×10⁻³ µg g⁻¹, respectively, with relative prediction errors below 5%, and a sample
22 throughput of about 8 samples per hour.
23
24
25
26
27
28
29
30
31
32
33
34
35
36
37
38
39
40
41
42
43
44
45
46
47
48
49
50
51
52
53
54
55
56
57
58
59
60

Introduction

Because of its high toxicity and stability in the aquatic environment, Hg(II) is considered as a priority pollutant.¹ This metal ion can be transformed via biotic and/or abiotic methylation into methyl mercury, a potent neurotoxin that concentrates through the food chain in the tissue of fishes. Subsequent ingestion by humans of seafood contaminated with this mercury derivative can cause adverse effects in vital organs and tissues, such as liver, brain and heart muscle.² Therefore, the concern of regulatory agencies to control the presence of Hg(II) and its derivatives in environmental samples is not surprising.³

Current analytical methods for mercury screening, including cold vapor atomic absorption spectroscopy⁴ and inductively coupled plasma-mass spectrometry⁵ require sophisticated and expensive equipment and frequently sample pre-processing steps. In the last decade, substantial efforts have been focused towards the development of fluorescent chemosensors and chemodosimeters for sensitive and selective routine monitoring of mercury in water and biological samples. Rhodamine⁶⁻¹² and 4,4-difluoro-4-bora-3a,4a-diaza-s-indacene or difluoroborondipyrromethene (BODIPY)¹³⁻¹⁸ derivatives are two of the most employed families of chemosensors for mercury detection. Culzoni et al. have reviewed both rhodamine and BODIPY-based fluorimetric sensors for Hg(II) ion, as applied to environmental and biochemical samples such as mineral, underground, river, pool, tap, lake and sea water samples, living cells, and fish samples.¹⁹ In this latter review, the structures of the numerous synthetic derivatives used as mercury sensors and their recognition mechanisms are discussed.

1
2
3 Specifically, BODIPY derivatives have several outstanding features, including
4 high fluorescence quantum yield and fine tunable spectroscopic properties.²⁰ Recently, a
5 chemosensor based on a BODIPY derivative armed with a tetraamide receptor
6 (BODIPYTD, see Fig. 1) was described for the fluorimetric determination of Hg(II) in
7 environmental water samples.¹⁸ While this particular derivative exhibits a weak
8 fluorescence emission intensity due to a deactivating photo–electron transfer (PET)
9 effect acting over the BODIPY core, an intense fluorescence signal is detected in the
10 presence of Hg(II). This increase in emission intensity was assigned to mercury
11 complex formation involving the nitrogen atoms of the receptor moiety, which blocks
12 the deactivating PET mechanism.¹⁸ Consequently, the system displays an intense OFF-
13 ON fluorescence enhancement, allowing the metal ion determination at very low
14 concentrations.
15
16
17
18
19
20
21
22
23
24
25
26
27
28
29
30

31 It was demonstrated that the fluorescence of this chemosensor, highly selective
32 towards Hg(II) ion, is not significantly affected by other competing metal ions such as
33 Li(I), Na(I), K(I), Ag(I), Mg(II), Ca(II), Ba(II), Fe(II), Fe(III), Cu(II), Zn(II), Cd(II),
34 Co(II), Pb(II), and Al(III), and successful Hg(II) recoveries were obtained in spiked tap
35 and waste water samples.¹⁸ However, it is likely that real environmental and
36 biochemical matrices will contain other fluorescent constituents (organic pollutants,
37 humic and fulvic acids, waste materials, degradation products, pharmaceuticals and
38 their metabolites, aminoacids, proteins, etc.) which could interfere in this
39 spectrofluorimetric determination, for example by displaying overlapping spectra. In
40 fact, the determination of contaminants in complex samples usually faces the problem
41 of the presence of interfering agents, which must be removed before quantification,
42 extending the analysis time and the experimental work. In addition, these separation
43
44
45
46
47
48
49
50
51
52
53
54
55
56
57
58
59
60

1
2
3 steps frequently involve the use of significant amounts of toxic organic solvents, in
4
5 disagreement with the green analytical chemistry principles.²¹
6
7

8 Therefore, a second-order multivariate calibration protocol using the presently
9
10 discussed BODIPYTD chemosensor is proposed in this work, as a useful approach for
11
12 the determination of Hg(II) ion in the presence of any expected or unexpected potential
13
14 interferences, with overlapping fluorescence excitation and/or emission spectra. Second-
15
16 order calibration allows reaching the second-order advantage,²² which refers to the
17
18 capacity of certain algorithms of allowing the accurate prediction of analyte
19
20 concentrations in complex samples containing potential interferences.²³ This useful
21
22 property avoids the requirement of interference removal, with the concomitant saving of
23
24 experimental work, analysis time, and use of toxic organic solvents required by clean-
25
26 up procedures.
27
28
29
30

31 Specifically, the algorithm known as parallel factor analysis (PARAFAC)²⁴ was
32
33 applied to the trilinear three-way data built with the excitation-emission fluorescence
34
35 matrices (EEFMs) generated by the BODIPYTD-Hg(II) complex under optimal
36
37 working conditions, and in the presence of other compounds selected as potential
38
39 interferences. The fitting of a trilinear three-way array to the PARAFAC model often
40
41 provides unique solutions, and the uniqueness of the decomposition is the natural basis
42
43 of the PARAFAC second-order advantage. The latter is the main advantage offered by
44
45 second-order calibration in comparison with the first-order counterpart.²²
46
47
48
49

50 It is interesting to note that this is the first time that second-order multivariate
51
52 calibration is applied in combination with a chemosensing system. A comparison with
53
54 other recently proposed schemes for Hg(II) detection is performed, and the feasibility of
55
56 determining Hg(II) ion in real environmental and biological matrices is demonstrated by
57
58
59
60

1
2
3 applying the proposed methodology to river and underground waters, and to fish muscle
4
5 tissues.
6
7
8
9

10 **Experimental**

11 **Reagents and solutions**

12
13 The synthesis of BODIPYTD (Fig. 1) and the confirmation of its structure by ^1H NMR
14
15 and ^{13}C NMR were performed as indicated in ref. 18. $\text{Hg}(\text{NO}_3)_2 \cdot \text{H}_2\text{O}$, methanol, nitric
16
17 acid and phosphate buffer were purchased from Merck (Darmstadt, Germany).
18
19 Riboflavin, erythrosine and acridine were of analytical grade and were used as received.
20
21
22
23

24
25 A stock solution of BODIPYTD ($1.50 \times 10^{-4} \text{ mol L}^{-1}$) was prepared in methanol,
26
27 and more diluted water solutions ($2.00 \times 10^{-5} \text{ mol L}^{-1}$) were prepared daily, taking an
28
29 appropriate volume from this methanol solution, evaporating the solvent with N_2 to
30
31 dryness, and diluting to the final volume with ultrapure water. The latter was obtained
32
33 from a Millipore Milli-Q system (Millipore, Bedford, MA).
34
35

36
37 A $\text{Hg}(\text{II})$ stock solution ($1.50 \times 10^{-3} \text{ mol L}^{-1}$) was prepared by dissolving
38
39 mercury(II) nitrate in doubly deionized water containing a few drops of concentrated
40
41 HNO_3 . More dilute sample solutions were prepared daily by appropriate dilution of the
42
43 stock solution with ultrapure water. A 0.5 mol L^{-1} phosphate buffer of $\text{pH}=7.50$ was
44
45 also prepared.
46
47
48

49
50 All stock solutions were stored in amber glass bottles at $4 \text{ }^\circ\text{C}$. Special care was
51
52 taken in the preparation and handling of solutions and containers to minimize any
53
54 possible risk of mercury contamination. Calibrated flasks were left overnight in 10%
55
56 (v/v) HNO_3 and rinsed with ultrapure Milli-Q water to eliminate contamination before
57
58 use.
59
60

Instrumentation

Fluorescence measurements were performed on a Varian Cary Eclipse (Varian, Mulgrave, Australia) luminescence spectrometer equipped with a 7 W Xenon pulse lamp and connected to a PC microcomputer. The data matrices were collected at excitation wavelengths from 470 to 510 nm each 2 nm, and emission wavelengths from 520 to 570 nm each 1 nm. Both excitation and emission slit widths were of 5 nm. The photomultiplier tube sensitivity was set at 800 V, and the scan rate was 600 nm min⁻¹. All measurements were carried out using a 1.00 cm quartz cell, thermostated at 18.0 ± 0.1 °C by means of an RM 6 LAUDA thermostatic bath.

Procedure

A calibration set of six samples were prepared by triplicate in the concentration range 0–100.0 ng mL⁻¹ by adding appropriate amounts of Hg(II) ion stock solution and 50.0 µL of 2.00×10⁻⁵ mol L⁻¹ BODIPYTD water solution into 2.00 mL volumetric flasks. After stirring for 5 minutes in the darkness, each solution was diluted to the mark with phosphate buffer (0.5 mol L⁻¹, pH=7.50), and the EEFM was collected and subjected to second-order data analysis. The time elapsed between consecutive measurements (including the stirring step and the fluorescence matrix measurement) was about 7.5 min. A validation set was similarly prepared, employing Hg(II) concentrations different than those used for calibration and following a random design, i.e., with concentrations taken at random from the corresponding calibration range.

As will be demonstrated below, the compounds riboflavin, erythrosine and acridine, chosen as model of potential contaminants, display fluorescence signals which significantly overlap with that for the studied Hg complex. Therefore, with the purpose of evaluating the proposed strategy in an interfering environment, twelve additional test

1
2
3 samples containing random concentrations of Hg(II) ion and the above mentioned three
4
5 compounds were prepared. The concentrations of the interfering agents in these latter
6
7 samples were in the ranges 50.0–200.0 ng mL⁻¹ for riboflavin and erythrosine, and
8
9 250.0–500.0 ng mL⁻¹ for acridine.
10
11

12 13 14 15 **Real samples**

16
17 Because all samples (waters and fishes) did not contain Hg(II) ion at levels higher than
18
19 the attained detection limit, a recovery study was carried out by spiking them with the
20
21 metal ion at different concentrations.
22
23
24
25

26 27 **Water samples**

28
29 A river water sample (Paraná River, Argentina) was collected near a region of high
30
31 industrial activity, and underground water samples were obtained from two different
32
33 cities (Venado Tuerto City and Santa Rosa City, Argentina) located at about 400 km
34
35 away from each other. In order to remove suspended solid materials, the evaluated river
36
37 and underground water samples were filtered through filter paper and through a nylon
38
39 membrane. To mimic a real situation, filtration was performed after the addition of the
40
41 Hg(II) standard solution. BODIPYTD aqueous solution was then added, and samples
42
43 were subjected, by duplicate, to the same procedure employed for the validation ones.
44
45
46
47
48
49

50 51 **Fish samples**

52
53 Fishes (tuna and mackerel) were collected from commercial markets. Three different
54
55 fish samples were tested: two tuna and one mackerel sample. A portion of the muscle
56
57 tissue was dried in an oven at 80 °C for 60 minutes. After grinding the dry tissue, 0.2000
58
59 g of each sample was weighed, spiked with the analyte, and digested in nitric acid at
60

1
2
3 100 °C for 100 minutes. The mixture was filtered with a paper disk into a volumetric
4 flask and diluted with phosphate buffer (0.5 mol L⁻¹, pH=7.50). The solution was then
5 filtered through a C18 membrane, BODIPYTD aqueous solution was added, and the
6 procedure described above was carried out. Each measurement was performed in
7 duplicate. It is necessary to point out that acid digestion is applied, and thus the organic
8 mercury species (e.g., methylmercury), if present, would render inorganic mercury,
9 which adds to the original Hg(II) ion contained in the sample. Therefore, the total
10 mercury content is determined following the proposed methodology.
11
12
13
14
15
16
17
18
19
20
21
22
23

24 **Software**

25
26 The theory of PARAFAC is well documented in the literature, and hence a brief
27 description is supplied in the Supplementary Data. The employed chemometric
28 algorithm (PARAFAC) was implemented in MATLAB 7.6,²⁵ using the codes provided
29 by Bro²⁶ and the MVC2 graphical interface,²⁷ which can be freely downloaded from
30 www.iquir-conicet.gov.ar/descargas/mvc2.rar. It is important to remark that analytical
31 readers not familiarized with chemometric analysis may find thorough explanations
32 about the MVC2 toolbox and the presently employed algorithm, including easily
33 understandable examples, in a recently published book.²⁸
34
35
36
37
38
39
40
41
42
43
44
45
46
47

48 **Results and discussion**

49 **Preliminary studies**

50
51 Exploratory experiments confirmed that the optimal conditions to obtain the best signal
52 were those indicated in a recent report.¹⁸ In fact, maximum fluorescence is observed
53 when the BODIPYTD and Hg²⁺ react in a 1:2 ratio under stirring for five minutes in the
54
55
56
57
58
59
60

1
2
3 darkness, and then phosphate buffer (pH=7.50) is added in order to stabilize the
4
5 fluorescence response of the complex.
6
7

8 Figure 2A shows the fluorescence excitation and emission spectra of
9
10 BODIPYTD in the absence and in the presence of increasing concentrations of Hg(II)
11
12 ion. As can be seen, the fluorescence signal increases with increasing concentrations of
13
14 the analyzed ion, and a slight shift to the red of the emission band (ca. 5 nm) is also
15
16 detected.
17
18
19
20
21

22 **Quantitative second-order analysis**

23 **Synthetic samples**

24
25 On the basis of the optimal conditions confirmed above, the spectrofluorimetric
26
27 determination of Hg(II) ion using the BODIPYTD chemosensor was carried out. As
28
29 previously demonstrated, the quantitation of the metal ion in matrices without organic
30
31 interferences was successfully performed through a direct univariate or zeroth-order
32
33 calibration.¹⁸ However, taking into account that environmental matrices may contain
34
35 interfering constituents, a second-order chemometric analysis was proposed. Although
36
37 the differences between excitation and emission spectra for free BODIPYTD and for the
38
39 mercury complex are not significant (Fig. 2B), the employed second-order algorithm
40
41 PARAFAC was able to distinguish these signals, rendering excellent results (see
42
43 below). Figure 2B shows the normalized excitation and emission fluorescence spectra
44
45 for free BODIPYTD in the absence and presence of Hg²⁺, and Fig. 2C displays the
46
47 corresponding results in the presence of riboflavin, erythrosine and acridine. Notice that
48
49 the profiles shown in Fig. 2B and 2C are normalized to unit length and do not represent
50
51 true intensities.
52
53
54
55
56
57
58
59
60

1
2
3 Initially, under the optimal working conditions, EEFMs were recorded for
4 calibration and validation samples, in the absence of additional compounds. Figure 3A
5 shows the three-dimensional plot and the corresponding contour plot for the EEFM of a
6 typical validation sample in the analyzed wavelength ranges.
7
8
9

10
11
12 PARAFAC was applied to three-way data arrays built by joining the calibration
13 data matrices with those for each of the validation samples in turn. The algorithm was
14 initialized with the loadings giving the best fit after a small number of trial runs,
15 selected from the comparison of the results provided by generalized rank annihilation
16 and several random loadings.²⁹ The number of components was selected by core
17 consistency analysis,³⁰ and also through visual inspection of the spectral profiles
18 produced by the addition of new components. If this addition generates repeated
19 profiles, suggesting overfitting, this new component was discarded. The number of
20 responsive components obtained in validation samples using both procedures was two,
21 justified by the presence of two different signals: those arising from the BODIPYTD-
22 Hg²⁺ complex and from free BODIPYTD. No restrictions were applied during
23 PARAFAC least-squares fit.
24
25
26
27
28
29
30
31
32
33
34
35
36
37
38
39
40

41 Figure 4A shows the prediction results after the application of PARAFAC to the
42 complete set of validation samples. As can be appreciated, the predictions for Hg(II)
43 concentrations are in good agreement with the nominal values. With the purpose of
44 assessing the accuracy of the predicted concentrations, the elliptical joint confidence
45 region (EJCR) test was performed.³¹ The EJCR test consists of plotting, in the slope-
46 intercept plane, the region of mutual confidence (usually at 95% confidence level) of the
47 slope and intercept for the regression of predicted vs. nominal concentrations. The
48 region has an elliptical shape, and the test consists in checking whether the theoretically
49 expected values of slope = 1 and intercept = 0 are included within the ellipse. When the
50
51
52
53
54
55
56
57
58
59
60

1
2
3 ideal point is included within the EJCR, this indicates accuracy of the used
4 methodology. Further details on the EJCR test can be found in the relevant literature.³¹
5

6
7
8 In the present case the ideal (1,0) point lies inside the EJCR surface (Fig. 4C),
9 suggesting that PARAFAC is appropriate for resolving the system under investigation.
10

11
12 The corresponding statistical results shown in Table 1 are also indicative of high-quality
13 predictions. The limit of detection (LOD) was estimated with the approach described in
14
15 ref. 32 according to the expression:
16
17

$$18 \quad \text{LOD} = 3.3 \sqrt{hs_C^2 + hs_X^2 / \text{SEN}^2 + s_X^2 / \text{SEN}^2} \quad (4)$$

19
20
21
22
23
24 where h is the sample leverage at zero analyte concentration, s_C^2 is the variance in
25 calibration concentrations, s_X^2 is the variance in the instrumental signal, SEN is the
26 component sensitivity, and the factor 3.3 is the sum of t -coefficients accounting for
27 types I and II errors (false detects and false non-detects, respectively) at 95 %
28 confidence level.³² Equation (4) takes into account the propagation of all possible error
29 sources (instrumental signal of the test sample, instrumental signal of calibration
30 samples, and calibration concentrations) to the predicted concentration error.³²
31
32
33

34
35
36
37
38
39
40
41 The obtained limit of detection ($\text{LOD} = 2 \text{ ng mL}^{-1}$) is significantly lower than
42 that obtained using the same BODIPYTD chemosensor, but applying univariate
43 calibration ($\text{LOD} = 5.5 \text{ ng mL}^{-1}$, ref. 18), and this is a clear demonstration of the
44 positive effect of the multivariate calibration on the sensitivity of the analysis.²³ The
45 relative error of prediction ($\text{REP} = 3 \%$) indicates a very good precision.
46
47
48
49
50
51

52
53 Because the real challenge is to obtain satisfactory predictions in systems where
54 other foreign compounds are also present, fluorescent compounds which may interfere
55 with the analysis were introduced in the test samples for evaluation. We found that the
56 excitation and emission spectra of certain compounds commonly found in natural
57
58
59
60

1
2
3 waters such as riboflavin, erythrosine and acridine are significantly overlapped with
4 those corresponding to the BODIPYTD-Hg²⁺ complex, producing a severe spectral
5 interference (Figs. 2C and 3B). Riboflavin (vitamin B2) is a well-known pigment
6 present in the waters of rivers, lakes and seas, which facilitates the photochemical
7 transformation of many pollutants in the environment,³³ erythrosine is a synthetic dye
8 used as a food additive frequently found in water as environmental pollutant,³⁴ and
9 acridine is often detected in natural waters because several dyes and drugs contain the
10 acridine skeleton. In fact, acridine is the major photodegradation intermediate of
11 carbamazepine which, in turn, is one of the most frequently found emerging
12 pharmaceutical contaminants.³⁵

13
14
15
16
17
18
19
20
21
22
23
24
25
26
27 In order to simulate a very unfavorable situation, the interferents were added at
28 high relative concentrations with respect to Hg(II). The number of responsible
29 components in these samples, selected by following a similar procedure to that indicated
30 above for the validation samples, was three. These PARAFAC components were
31 assigned to: (1) the mercury complex, (2) free BODIPYTD and (3) a combined signal
32 corresponding to the interferents. Apparently, PARAFAC is not able to discern between
33 the profiles of each individual foreign compound, and retrieves the interfering profile as
34 a single unexpected mathematical component. However, this fact does not preclude the
35 obtainment of good analytical results in these complex samples (Fig. 4B),
36 demonstrating the high level of selectivity achieved by this method.
37
38
39
40
41
42
43
44
45
46
47
48
49

50
51 The statistical results shown in Table 1 also support this conclusion, implying
52 good values for the root mean square error of prediction (RMSEP) and REP. The LODs
53 obtained both in the absence and presence of interferents (2 and 4 ng mL⁻¹,
54 respectively) are acceptable, taking into account that a very simple methodology is
55
56
57
58
59
60

1
2
3 applied to rather complex samples. It is necessary to recall that this limits have been
4
5 calculated using the strict expressions recommended by IUPAC,³² as indicated above.
6
7
8
9

10 **Real samples**

11
12 The applicability of the proposed method was tested spiking with the analyte both water
13 and fish samples found to be free from Hg(II) ion, and performing recovery studies.
14
15 Figures 3C and 3D show three-dimensional plots of the EEFMs and the corresponding
16
17 contour plots for samples of river water and tuna fish, both spiked with Hg²⁺. In
18
19 comparing these figures with that of a typical validation sample (without spectral
20
21 interferences), it is apparent that a zeroth-order (univariate) calibration could not be
22
23 applied, unless a severe sample pretreatment for removing the contribution of matrix
24
25 interferences is employed. However, pretreatment steps are not necessary or minimal
26
27 when using second-order calibration, as in the present case.
28
29
30
31
32
33

34 The results provided by PARAFAC for the studied water samples (Table 2) are
35
36 outstanding, suggesting that the method can overcome the problem of the presence of
37
38 unexpected interferences (both metal ions and organic compounds) from environmental
39
40 background matrices.
41
42

43 Table 1 summarizes the corresponding figures of merit obtained for these water
44
45 samples. The obtained LOD is equal to that obtained for validation samples, indicating
46
47 that the presence of additional constituents does not decrease the sensitivity of the
48
49 method. Although the United State Environmental Protection Agency (US EPA)³⁶ has
50
51 set a maximum contaminant level of Hg(II) in drinking water at 2 ng mL⁻¹, and a
52
53 tolerance limit in surface water of 10 ng mL⁻¹,³⁷ higher concentrations can be detected
54
55 (> 50 ng mL⁻¹) in industrial wastewaters.^{18,38} As a conclusion, the LOD calculated
56
57 applying the present methodology is appropriate for determining Hg (II) ion in
58
59
60

1
2
3 environmental samples (surface waters and industrial wastewaters), as suggested by the
4
5 US EPA, with the advantage that it was obtained applying a simple method with a
6
7 minimal sample treatment, and without using organic solvents. The above described
8
9 EJCR test was applied to these samples (data not shown) and the obtained result, with
10
11 the theoretically expected values of slope = 1 and intercept = 0 included within the
12
13 corresponding ellipse, corroborates the accuracy of the method.
14
15

16
17 The recovery results obtained for fish samples (Table 3), the corresponding
18
19 EJCR test (data not shown) and the remaining statistical results (Table 1) were also very
20
21 satisfactory. The US EPA has established a level of $0.55 \mu\text{g g}^{-1}$ of mercury in edible
22
23 fish tissues.³⁹ On the other hand, the current allowable mercury level in commercial fish
24
25 and fisheries products directed by the United State Food and Drug Administration (US
26
27 FDA)⁴⁰ is $1.0 \mu\text{g g}^{-1}$. Therefore, the LOD value achieved through the proposed method
28
29 (LOD = $4 \times 10^{-3} \mu\text{g g}^{-1}$) is significantly lower than the above established levels,
30
31 corroborating the usefulness of the method for the Hg(II) determination in this type of
32
33 samples.
34
35

36
37 As indicated in the introduction, a significant number of reports describing the
38
39 development of Hg(II) chemosensors using different strategies has been published. An
40
41 original approach that should be mentioned is based on the fluorescence quenching
42
43 effect of Hg(II) on CdS quantum dots-dendrimer nanocomposites. PARAFAC was
44
45 employed for confirming the mechanism of action.⁴¹
46
47
48

49
50 In Table 4, important analytical characteristics of relevant chemosensors
51
52 recently reported for the determination of Hg^{2+} are summarized and compared with the
53
54 method here proposed. The reported LODs of the selected methods range from 0.4 to
55
56 200 ng mL^{-1} . It is important to take into account that these values were in general
57
58 calculated as three times the standard deviation of the blank signal, yielding therefore
59
60

1
2
3 more favorable values, although they do not comply with the latest IUPAC
4
5 recommendations.³²
6
7

8 The selectivity of the proposed method, which employs second-order calibration
9
10 with the concomitant second-order advantage (see above), favorably compares with
11
12 those using the traditional zeroth-order calibration, which could not overcome the
13
14 problem of spectral interference from organic species. Finally, the fact that the
15
16 experiments are carried out in aqueous solutions adds to the advantages of the proposed
17
18 method.
19
20
21
22
23
24

25 **Conclusions**

26
27 A novel and environmentally friendly method for Hg(II) ion determination was
28
29 described, using a fluorescence chemosensor based on a boron dipyrromethene
30
31 tetraamine derivative (BODIPYTD) in combination with second-order multivariate
32
33 calibration. Excitation-emission fluorescence matrices for the BODIPYTD-mercury
34
35 complex were processed by PARAFAC, allowing the successful determination of the
36
37 metal ion at levels required by regulatory agencies. The novelty of the proposed
38
39 approach rests in the fact that it enabled determination of trace levels of the pollutant
40
41 metal ion, even in the presence of potential organic interferences which display
42
43 fluorescence signals in the same spectral range as the studied chemosensing mercury
44
45 complex. The application of a chemometric tool makes it unnecessary to apply
46
47 additional clean up steps for the removal of interfering compounds, saving experimental
48
49 time and operator efforts, and avoiding the use of contaminating solvents. The obtained
50
51 results suggest that the proposed approach is suitable for the analysis of mercury ion in
52
53 environmental samples, favorably competing with current methods, without requiring
54
55 expensive and sophisticated equipment and clean up procedures. The combined gains in
56
57
58
59
60

1
2
3 selectivity towards inorganic and organic interferents presage auspicious applications of
4 chemosensors coupled to multivariate calibration in analytical laboratories.
5
6
7
8
9

10 **Acknowledgements**

11
12 The authors are grateful to the Universidad Nacional de Rosario, and Consejo Nacional
13 de Investigaciones Científicas y Técnicas (CONICET), and Ministerio de Economía y
14 Competitividad of Spain (Proyect CTQ2011-25388) and Gobierno de Extremadura
15 (Proyect GR1003-FQM003), both co-financed by European FEDER funds, for
16 financially supporting this work.
17
18
19
20
21
22
23
24
25
26
27

28 **References**

- 29
30
31 1 Website of the United State Environmental Protection Agency (U.S. EPA),
32 Priority pollutants, <http://water.epa.gov/scitech/methods/cwa/pollutants.cfm>.
33
34 2 J. G. Dórea, *Sci. Total Environ.*, 2008, **400**, 93–114.
35
36 3 K. Leopold, M. Foulkes and P. Worsfold, *Anal. Chim. Acta*, 2010, **663**, 127–
37 138.
38
39 4 V. Azevedo Lemos and L. Oliveira dos Santos, *Food Chem.*, 2014, **149**, 203–
40 207.
41
42 5 Y. Gao, Z. Shi, Q. Zong, P. Wu, J. Su and R. Liu, *Anal. Chim. Acta*, 2014, **812**,
43 6–11.
44
45 6 J. Luo, S. Jiang, S. Qin, H. Wu, Y. Wang, J. Jiang and X. Liu, *Sens. Actuators B*,
46 2011, **160**, 1191–1197.
47
48 7 J. Zhang, Y. Zhou, W. Hu, L. Zhang, Q. Huang and T. Ma, *Sens. Actuators B*,
49 2013, **183**, 290–296.
50
51
52
53
54
55
56
57
58
59
60

- 1
2
3
4 8 D. Wu, Z. Wang, G. Wu and W. Huang, *Mater. Chem. Phys.*, 2012, **137**, 428–
5
6 433.
7
8
9 9 D. Bohoyo Gil, M. I. Rodríguez-Cáceres, M. C. Hurtado-Sánchez and A.
10
11 Muñoz de la Peña, *Appl. Spectrosc.*, 2010, **64**, 520–527.
12
13 10 V. A. Lozano, G. M. Escandar, M. C. Mahedero and A. Muñoz de la Peña, *Anal.*
14
15 *Methods*, 2012, **4**, 2002–2008.
16
17 11 X. C. Fu, J. Wu, C. G. Xie, Y. Zhong and J. H. Liu, *Anal. Methods*, 2013, **5**,
18
19 2615–2622.
20
21 12 X. Zhang and Y. Y. Zhu, *Sens. Actuators B*, 2014, **202**, 609–614.
22
23 13 S. Atilgan, I. Kutuk and T. Ozdemir, *Tetrahedron Lett.*, 2010, **51**, 892–894.
24
25 14 D. Kim, K. Yamamoto and K. H. Ahn, *Tetrahedron*, 2012, **68**, 5279–5282.
26
27 15 T. K. Khan and M. Ravikanth, *Dyes Pigm.*, 2012, **95**, 89–95.
28
29 16 A. N. Kursunlu, P. Deveci and E. Guler, *J. Luminesc.*, 2013, **136**, 430–436.
30
31 17 J. Fan, X. Peng, S. Wang, X. Liu, H. Li and S. Sun, *J. Fluoresc.*, 2012, **22**, 945–
32
33 951.
34
35 18 M. J. Culzoni, A. Muñoz de la Peña, A. Machuca, H. C. Goicoechea, R. Brasca
36
37 and R. Babiano, *Talanta*, 2013, **117**, 288–296.
38
39 19 M. J. Culzoni, A. Muñoz de la Peña, A. Machuca, H. C. Goicoechea, R. Brasca
40
41 and R. Babiano, *Anal. Methods*, 2013, **5**, 30–49.
42
43 20 F. Han, Y. Xu, D. Jiang, Y. Qin and H. Chen, *Anal. Biochem.*, 2013, **435**, 106–
44
45 113.
46
47 21 A. Gałuszka, Z. Migaszewski and J. Namieśnik, *Trends Anal. Chem.*, 2013, **50**,
48
49 78–84.
50
51 22 K. S. Booksh and B. R. Kowalski, *Anal. Chem.*, 1994, **66**, 782A–791A.
52
53
54
55
56
57
58
59
60

- 1
2
3
4 23 G. M. Escandar, H. C. Goicoechea, A. Muñoz de la Peña and A. C. Olivieri,
5
6 *Anal. Chim. Acta*, 2014, **806**, 8–26.
7
8
9 24 R. Bro, *Chemom. Intell. Lab. Syst.*, 1997, **38**, 149–171.
10
11 25 MATLAB R2011b, The MathWorks Inc., Natick, MA, USA.
12
13 26 <http://www.models.life.ku.dk/algorithms>.
14
15
16 27 A. C. Olivieri, H. L. Wu and R. Q. Yu, *Chemom. Intell. Lab. Syst.*, 2009, **96**,
17
18 246–251.
19
20 28 A. C. Olivieri and G. M. Escandar, *Practical three-way calibration*, Elsevier,
21
22 Waltham, USA, 2014.
23
24
25 29 P. C. Damiani, I. Durán Merás, A. García Reiriz, A. Jiménez Jirón, A. Muñoz de
26
27 la Peña and A. C. Olivieri, *Anal. Chem.*, 2007, **79**, 6949–6958.
28
29
30 30 R. Bro and H. A. L. Kiers, *J. Chemom.*, 2003, **17**, 274–286.
31
32 31 A. G. González, M. A. Herrador and A. G. Asuero, *Talanta*, 1999, **48**, 729–736.
33
34 32 A. C. Olivieri, *Chem. Rev.*, 2014, **114**, 5358–5378.
35
36 33 X. Zhao, X. Hu and H. M. Hwang, *Chemosphere*, 2006, **63**, 1116–1123.
37
38 34 Y. S. Al-Degs, R. A. El-Halawa, and S. S. Abu-Alrub, *Chem. Eng. J.*, 2012, **191**,
39
40 185–194.
41
42
43 35 S. Chiron, C. Minero and D. Vione, *Environ. Sci. Technol.*, 2006, **40**, 5977–
44
45 5983.
46
47
48 36 Website of the United State Environmental Protection Agency (U.S. EPA),
49
50 Water: historical archive of drinking water contaminant fact sheets,
51
52 <http://water.epa.gov/drink/contaminants/basicinformation/mercury.cfm>.
53
54
55 37 M. K. Hafshejani, A. Vahdati, M. Vahdati, A.B. Kheradmand, M. Sattari, A.
56
57 Arad and S. Choopani, *Life Sci. J.*, 2012, **9**, 1846–1848.
58
59
60

- 1
2
3
4 38 M. G. Afshar, M. Soleimani and M. Bazrpach, *World Acad. Sci. Eng. Techn.*,
5
6 2011, **5**, 283–284.
7
8
9 39 US-EPA, Regulatory impact analysis of the clean air Mercury rule: EPA-452/R-
10
11 05-003, 2005.
12
13 40 J. M. Hightower and D. L Brown, *Environ. Health*, 2011, **10**, doi:10.1186/1476-
14
15 069X-10-90.
16
17
18 41 B. B. Campos, M. Algarra, B. Alonso, C. M. Casado and J.C.G. Esteves da
19
20 Silva, *Analyst*, 2009, **134**, 2447–2452.
21
22
23
24
25
26
27
28
29
30
31
32
33
34
35
36
37
38
39
40
41
42
43
44
45
46
47
48
49
50
51
52
53
54
55
56
57
58
59
60

Table 1 Statistical results for Hg(II) in synthetic and real samples

	Validation ^a	Test ^b	Water ^c		Fish ^d
LOD ^e (ng mL ⁻¹)	2	4	2	LOD ^e (μg g ⁻¹)	4×10 ⁻³
LOQ ^f (ng mL ⁻¹)	6	12	6	LOQ ^f (μg g ⁻¹)	1.2×10 ⁻²
RMSEP ^g (ng mL ⁻¹)	2	2	2	RMSEP ^g (μg g ⁻¹)	2×10 ⁻³
REP ^h (%)	3	5	3	REP ^h (%)	4
(R ²) ⁱ	0.9989	0.9928	0.9961	(R ²) ⁱ	0.9932

^a Twelve samples. ^b Twelve samples containing riboflavin, erythrosine and acridine as interferences. ^c Three different natural waters evaluated at three Hg(II) levels each.

^d Three different muscle tissue of fish (tuna and mackerel) samples evaluated at two Hg(II) levels each. ^e LOD, limit of detection calculated according to ref. 32. ^f LOQ, limit of quantitation calculated as LOD×(10/3.3). ^g RMSEP, root-mean-square error of prediction. ^h REP, relative error of prediction. ⁱ R², correlation coefficient.

Table 2 Recovery study of Hg(II) for spiked water samples using PARAFAC

Sample	Taken (ng mL ⁻¹)	Found (ng mL ⁻¹) ^a	Recovery (%)
River water	10.0	10 (2)	100
(Paraná River)	20.0	21 (3)	105
	30.0	34 (1)	112
Underground water	10.0	10 (1)	100
(Venado Tuerto City)	20.0	20 (1)	100
	30.0	31 (1)	103
Underground water	10.0	10 (1)	100
(Santa Rosa City)	20.0	19 (3)	95
	30.0	32 (2)	107

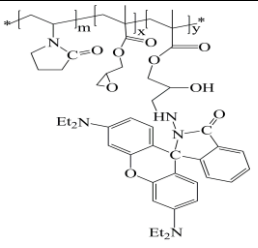
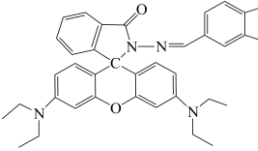
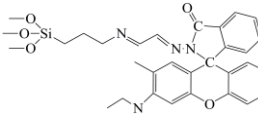
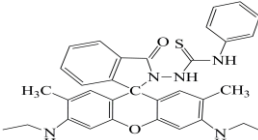
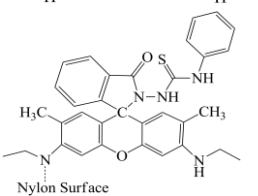
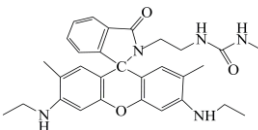
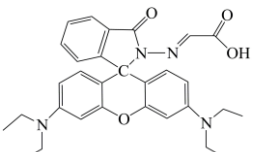
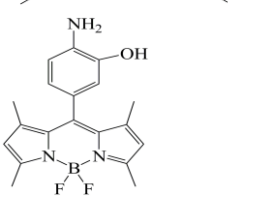
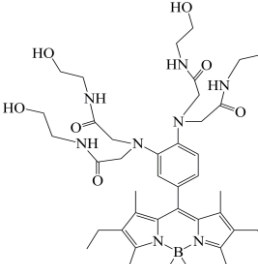
^a Mean of two determinations. Standard deviations between parentheses.

Table 3 Recovery study of Hg(II) for spiked fish samples using PARAFAC

Sample ^a	Taken ($\mu\text{g g}^{-1}$)	Found ($\mu\text{g g}^{-1}$) ^b	Recovery (%)
Tuna #1	0.12	0.11 (0.01)	93
	0.30	0.36 (0.02)	120
Tuna #2	0.12	0.10 (0.01)	83
	0.30	0.27 (0.01)	90
Mackerel	0.12	0.11 (0.01)	92
	0.30	0.31 (0.01)	103

^a Tuna #1 and #2 refer to two different specimens of tuna fish. ^b Mean of two determinations. Standard deviations between parentheses.

Table 4 Analytical performance of selected chemosensors recently reported for the determination of Hg(II) ion

Sensor ^a	Chemical structure	Reaction medium	Calibration data order	LOD ^b	Sample	Ref.
RD1		Aqueos	Zeroth-	10	Water	6
RD2		Aqueos	Zeroth-	2.4	Water	7
RD3		Aqueos	Zeroth-	2	Water	8
RD4		Organic	Zeroth-	0.7 ^d	Water, fish	9
RD5		Aqueos	Zeroth-	0.4	Water	10
RD6		Organic	Zeroth-	20	Water	11
RD7		Aqueos	Zeroth-	200	Water	12
BD1		Organic	Zeroth-	≤ 2	Water	17
BD2		Aqueos	Zeroth-	5.5	Water	18
BD3	Idem BD2	Aqueos	Second- ^c	2 ^d	Water, fish	This work

^a RD = rhodamine derivative, BD = BODIPY derivative. ^b LODs are given in ng mL⁻¹. ^c In the presence of organic interferents (see text). ^d LOD refers to water samples.

Figure Captions

Fig. 1 Structure of BODIPYTD: 4,4-difluoro-8-(aryl)-1,3,5,7-tetramethyl-2,6-diethyl-4-bora-3a,4a-diaza-*s*-indacene, where aryl = 3,4-(bis((bis(2-(2-hydroxyethyl)amino)-2-oxoethyl)amino))phenyl.

Fig. 2 (A) Excitation and emission fluorescence spectra for the free BODIPY derivative (dashed red lines) and for the BODIPY derivative in the presence of 20, 40, 60, 80 and 100 ng mL⁻¹ Hg(II) ion (solid lines). (B) Normalized excitation and emission fluorescence spectra for the free BODIPY derivative (dashed red lines) and for the BODIPY derivative-Hg²⁺ complex (black lines). (C) Normalized excitation and emission fluorescence spectra for the BODIPY-Hg²⁺ complex (black lines), riboflavin (green lines), erythrosine (cyan lines) and acridine (pink lines) under the applied experimental conditions (pH = 7.5).

Fig. 3 Three-dimensional plots and the corresponding contour plots of excitation-emission matrices for (A) a validation sample containing 21.0 ng mL⁻¹ Hg(II), (B) a test sample containing 18.0 ng mL⁻¹ Hg(II), 100 ng mL⁻¹ riboflavin, 100 ng mL⁻¹ erythrosine and 250 ng mL⁻¹ acridine, (C) a spiked river sample ($C_{\text{Hg(II)}} = 16.2 \text{ ng mL}^{-1}$), and (D) a spiked tuna fish sample after nitric acid treatment ($C_{\text{Hg(II)}} = 15 \text{ ng mL}^{-1}$). In all cases $C_{\text{BODIPYTD}} = 2.00 \times 10^{-5} \text{ mol L}^{-1}$.

Fig. 4 Plots of PARAFAC Hg(II) predicted concentrations as a function of the nominal values for validation samples (A), and for samples with interferences (test samples) (B). In (A) and (B) the solid lines are the perfect fits. (C) Elliptical joint regions (at 95 % confidence level) for slopes and intercepts of the regression for validation (blue line) and for test (red line) samples. The black circle marks the theoretical (intercept = 0, slope = 1) point.

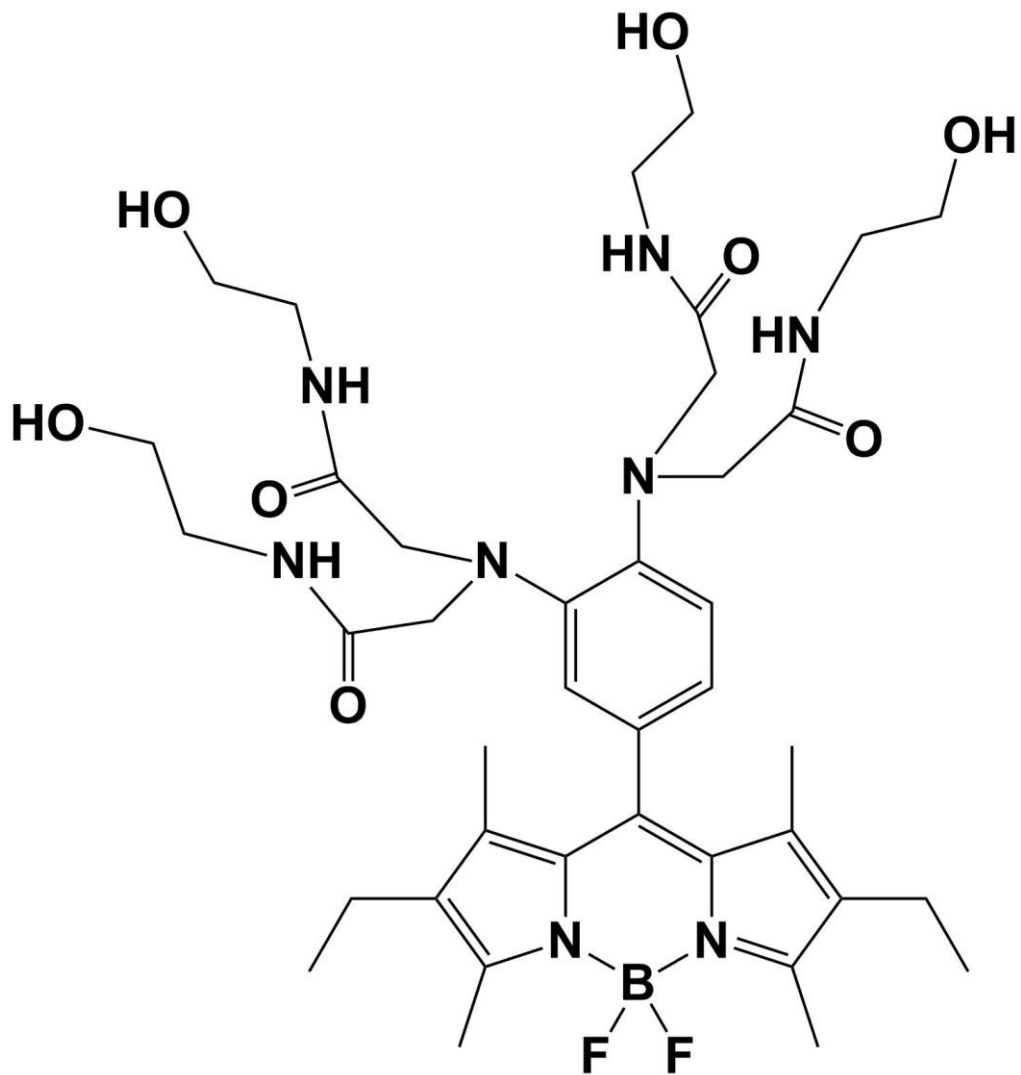


FIGURE 1

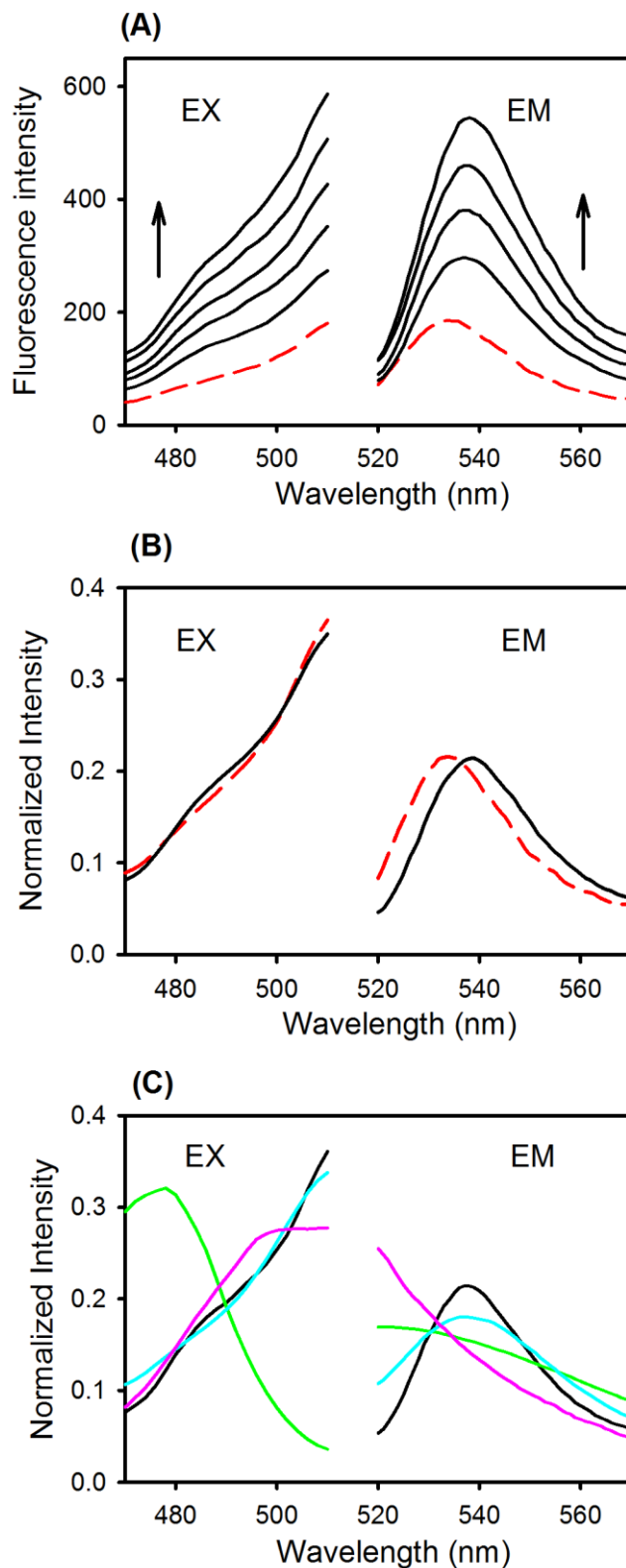


FIGURE 2

Analytical Methods

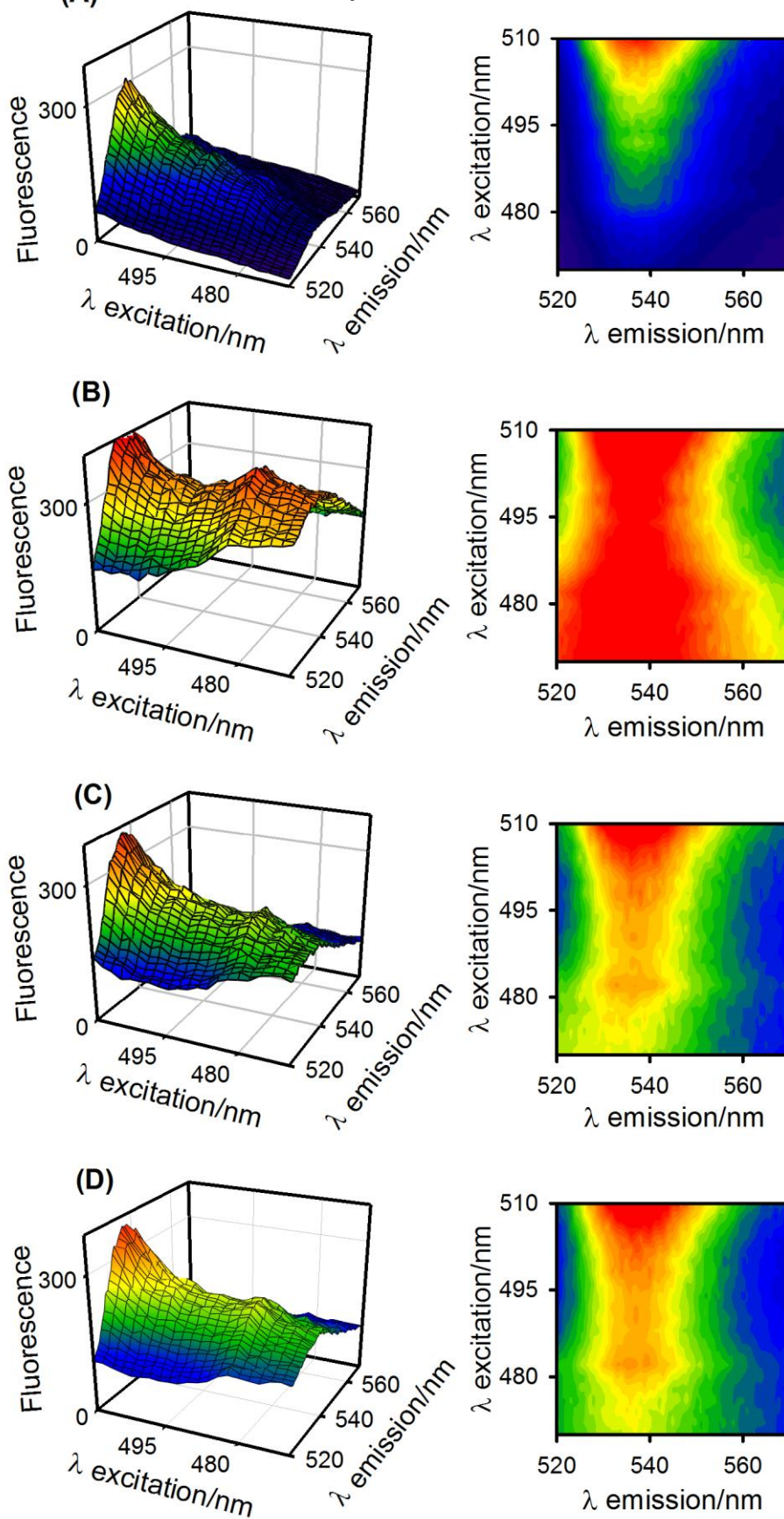


FIGURE 3

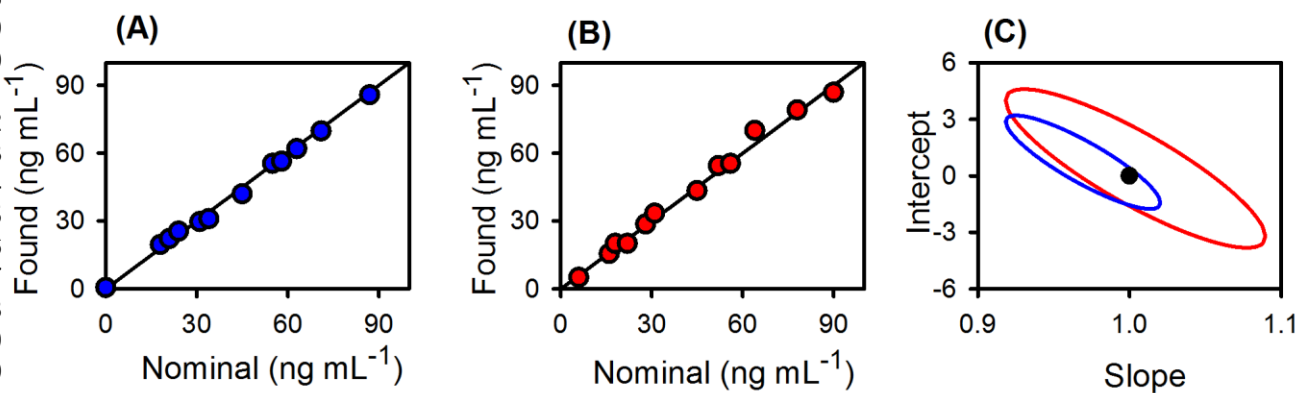


FIGURE 4